

Wilson coefficients for Higgs boson production and decoupling relations to $\mathcal{O}(\alpha_s^4)$

Marvin Gerlach, Florian Herren and Matthias Steinhauser

*Institut für Theoretische Teilchenphysik
Karlsruhe Institute of Technology (KIT)
76128 Karlsruhe, Germany*

Abstract

An important ingredient for the calculation of Higgs boson properties in the infinite top quark mass limit is the knowledge of the effective coupling between the Higgs bosons and gluons, i.e. the Wilson coefficients C_H and C_{HH} for one and two Higgs bosons, respectively. In this work we calculate for the first time C_{HH} to four loops in a direct, diagrammatic way, discussing in detail all issues arising due to the renormalization of operator products. Furthermore, we also calculate the Wilson coefficient C_H for the coupling of a single Higgs boson to gluons as well as all four loop decoupling relations in QCD with general $SU(N_c)$ colour factors. The latter are related to C_H and C_{HH} via low-energy theorems.

1 Introduction

In the coming years the production and decay of Higgs bosons will play a central role in many analyses performed at the Large Hadron Collider (LHC). A crucial ingredient is often provided by the matching coefficients which govern the coupling of Higgs bosons to gluons. The corresponding effective Lagrange density is valid in the heavy top quark limit which provides a good approximation for Higgs boson decays to gluons and the total production cross section of a single Higgs boson. For less inclusive processes the applicability of the effective theory approach is limited to parts of the phase space. This is also true for Higgs boson pair production. In this paper we perform for the first time a direct calculation of the matching coefficient for the coupling of one and two Higgs bosons to gluons. Our results are expressed in terms of general $SU(N_c)$ colour factors. For $N_c = 3$ they can be compared to expressions obtained from indirect methods where the matching coefficients are obtained from low-energy theorems (LETs). The essential ingredient into the LETs is the QCD decoupling constant for the strong coupling. For this reason we re-visit the calculation of all four-loop decoupling constants and provide results for a generic $SU(N_c)$ gauge group.

The remainder of this paper is organized as follows: In Section 2 we fix our notation and introduce the decoupling constants and the effective Lagrange density for the Higgs-gluon coupling. In Sections 3 and 4 we present our results for the decoupling relations and Wilson coefficients, respectively. We discuss in detail the extraction of the coupling of two Higgs bosons to gluons (C_{HH}) and in particular the subtleties in the matching procedure due to the renormalization of products of operators. Our findings are summarized in Section 5. In the Appendix we collect analytic results for the decoupling constants.

2 Technicalities

For convenience of the reader and to fix our notation we repeat in this Section the definition of the decoupling constants in QCD and the Wilson coefficients in the effective Lagrange density describing Higgs-gluon couplings. For a detailed discussion we refer to Ref. [1]. We will work in the $\overline{\text{MS}}$ scheme throughout this paper, except for the heavy quark mass which we renormalize both in the $\overline{\text{MS}}$ and on-shell scheme. The $\overline{\text{MS}}$ counterterms are needed up to four-loop order (see, e.g., Ref. [2]) and the renormalization constant for the $\overline{\text{MS}}$ to on-shell conversion for the heavy quark mass to three loops [3–6].

2.1 Decoupling constants

The bare and renormalized parameters and fields of the QCD Lagrangian are connected by renormalization constants defined through

$$g_s^0 = \mu^\epsilon Z_g g_s, \quad m_q^0 = Z_m m_q, \quad \xi^0 - 1 = Z_3(\xi - 1),$$

$$A_\mu^{0,a} = \sqrt{Z_3} A_\mu^a, \quad \psi_q^0 = \sqrt{Z_2} \psi_q, \quad c^{0,a} = \sqrt{\tilde{Z}_3} c^a. \quad (1)$$

Here g_s is the QCD gauge coupling with $\alpha_s = g_s^2/(4\pi)$ being the strong coupling constant, μ is the renormalization scale, $D = 4 - 2\epsilon$ the space-time dimension and ξ the gauge parameter with $\xi = 0$ corresponding to Feynman and $\xi = 1$ to Landau gauge. The gluon field is given by A_μ^a , ψ_q is the quark field of flavour q with mass m_q and c^a is the ghost field. Bare quantities are denoted by the superscript “0”. The renormalization constants Z_X are needed up to $\mathcal{O}(\alpha_s^4)$ [2, 7–10] for our purposes.

In the following we assume a strong hierarchy in the quark masses and integrate out a heavy quark with mass m_h from QCD with n_f active quark flavours.¹ The resulting effective Lagrangian has the same form as the original QCD Lagrangian. However, it only has $n_l = n_f - 1$ active quark flavours and thus only depends on the light degrees of freedom. The parameters and fields in the effective n_l -flavour and full n_f -flavour theory are related via the so-called (bare) decoupling constants

$$\begin{aligned} g_s^{0(n_l)} &= \zeta_g^0 g_s^{0(n_f)}, & m_q^{0(n_l)} &= \zeta_m^{0(n_f)} m_q^0, & \xi^{0(n_l)} - 1 &= \zeta_\xi^0 (\xi^{0(n_f)} - 1), \\ A_\mu^{0(n_l)} &= \sqrt{\zeta_3^0} A_\mu^{0(n_f)}, & \psi_q^{0(n_l)} &= \sqrt{\zeta_2^0} \psi_q^{0(n_f)}, & c^{0(n_l)} &= \sqrt{\tilde{\zeta}_3^0} c^{0(n_f)}, \end{aligned} \quad (2)$$

where the superscripts denote the number of active quark flavours. For simplicity we refrain to show colour indices for the fields. The different decoupling constants ζ_X contain the radiative effects of the heavy quark and can be computed in a perturbative series in α_s .

One obtains the renormalized decoupling constants by replacing the bare parameters and fields in Eq. (2) by renormalized counterparts using Eq. (1). As an example, consider the gauge coupling where the renormalized decoupling constant is given by

$$g_s^{(n_l)} = \frac{Z_g^{(n_f)}}{Z_g^{(n_l)}} \zeta_g^0 g_s^{(n_f)} = \zeta_g g_s^{(n_f)}. \quad (3)$$

Note that $Z_g^{(n_l)}$ depends on $g_s^{(n_l)}$ which has to be transformed to $g_s^{(n_f)}$ using Eq. (3). Thus, it is natural to apply Eq. (3) iteratively to arrive at four loops. Note that the loop corrections to the renormalization constants only contain poles whereas the decoupling constants also contain positive powers in ϵ . Thus, $Z_g^{(n_l)}$ expressed in terms of $g_s^{(n_f)}$ also contains positive powers in ϵ .

For later convenience we define the decoupling constant for the strong coupling constant α_s as

$$\zeta_{\alpha_s} = \zeta_g^2. \quad (4)$$

¹The simultaneous decoupling of two heavy quarks with different masses is discussed in Ref. [11] up to three-loop order.

2.2 Wilson coefficients for Higgs boson production and decay

In the Standard Model, the coupling of a Higgs boson to gluons is mainly mediated by top quark loops and thus in the following we have $n_f = 6$ and $n_l = 5$ for the full and effective theory, respectively. The effective Lagrange density which describes the coupling of one or two Higgs boson to gluons is obtained after integrating out the top quark and is given by

$$\mathcal{L}_{\text{eff}} = -\frac{H}{v} C_H^0 \mathcal{O}_1^0 + \frac{1}{2} \left(\frac{H}{v} \right)^2 C_{HH}^0 \mathcal{O}_1^0, \quad (5)$$

where $\mathcal{O}_1 = G_{\mu\nu}^a G^{\mu\nu,a}/4$, with $G_{\mu\nu}^a$ being the gluon field strength tensor, is the only physical operator one has to consider. It is defined in the $n_l = 5$ -flavour effective theory. The Wilson coefficients C_H^0 and C_{HH}^0 comprise the radiative effects of the top quark, which is in analogy to the decoupling constants introduced in Eq. (2).

The renormalization of \mathcal{O}_1 has been discussed in detail in Ref. [12] (see also Ref. [13]). In fact, the renormalization constant $Z_{\mathcal{O}_1}$ can be expressed through the QCD beta function through all orders in perturbation theory [12]

$$Z_{\mathcal{O}_1} = \frac{1}{1 - \beta(\alpha_s^{(5)})/\epsilon}, \quad (6)$$

with

$$\begin{aligned} \beta(\alpha_s) &= -\left(\frac{\alpha_s}{\pi}\right)^2 \sum_{n \geq 0} \beta_n \left(\frac{\alpha_s}{\pi}\right)^n, \\ \beta_0 &= \frac{1}{4} \left(\frac{11}{3} C_A - \frac{4}{3} T_F n_f \right), \\ \beta_1 &= \frac{1}{16} \left(\frac{34}{3} C_A^2 - \frac{20}{3} C_A T_F n_f - 4 C_F T_F n_f \right), \\ \beta_2 &= \frac{1}{64} \left(\frac{2857}{54} C_A^3 - \frac{1415}{27} C_A^2 T_F n_f - \frac{205}{9} C_A C_F T_F n_f + 2 C_F^2 T_F n_f \right. \\ &\quad \left. + \frac{158}{27} C_A T_F^2 n_f^2 + \frac{44}{9} C_F T_F^2 n_f^2 \right). \end{aligned} \quad (7)$$

$Z_{\mathcal{O}_1}$ can be used to obtain the renormalized Wilson coefficients via the relation

$$C_X^0 \mathcal{O}_1^0 = \frac{C_X^0}{Z_{\mathcal{O}_1}} Z_{\mathcal{O}_1} \mathcal{O}_1^0 = C_X \mathcal{O}_1, \quad (8)$$

with $X \in \{H, HH\}$.

2.3 Low energy theorems

There is a close connection between the decoupling constants from Subsection 2.1 and the Wilson coefficients from 2.2 which is established by the so-called LETs. In [1] a LET relating ζ_{α_s} and C_H has been derived

$$C_H = -\frac{m_t}{\zeta_{\alpha_s}} \frac{\partial}{\partial m_t} \zeta_{\alpha_s} \quad (9)$$

where we adapted the prefactors to match our conventions. Beyond three loops C_H has only been obtained with the help of Eq. (9). In this work we perform an explicit calculation of C_H for general $SU(N_c)$ colour factors.

Recently, in Ref. [14] a LET has been proposed for C_{HH} which reads

$$C_{HH} = \frac{m_t^2}{\zeta_{\alpha_s}} \frac{\partial^2}{\partial m_t^2} \zeta_{\alpha_s} - 2 \left(\frac{m_t}{\zeta_{\alpha_s}} \frac{\partial}{\partial m_t} \zeta_{\alpha_s} \right)^2. \quad (10)$$

It provides the correct result for C_{HH} at three-loop order [15]; in Section 4 we perform an explicit calculation of C_{HH} and show that Eq. (10) also works at four loops.

Note that in QCD ζ_{α_s} depends on m_t only via logarithms of the form $\log(\mu^2/m_t^2)$. Thus, it is possible to reconstruct the m_t dependence at $(n+1)$ -loop order from the n -loop result of ζ_{α_s} with the help of renormalization group equations. Using the LETs this immediately leads to the $(n+1)$ -loop results for C_H and C_{HH} .

2.4 Computational setup

For our calculation we use a well tested, automated setup, starting with the generation of Feynman diagrams using `qgraf` [16]. The output is processed by `q2e` and `exp` [17–19], which generate `FORM` [20] code for the amplitudes and map them onto individual integral families. We then compute the colour factors of the diagrams using `color` [21] and combine amplitudes with the same colour factors and integral families to so-called superdiagrams so that we can process them together.

After processing Lorentz structures and expanding in the external momenta, we are left with single-scale tensor tadpole integrals. We perform a tensor decomposition and reduce the remaining, scalar integrals to master integrals, using `LiteRed` [22, 23] and `FIRE5` [24]. With the help of the `FindRules` command of `FIRE5` we identify equivalent master integrals from different integral families.

The master integrals are all known to sufficiently high order in ϵ [25] (see also [26, 27]). The missing ϵ^3 term of the integral $J_{6,2}$ (in the notation of [25]) was provided in [28].

As a cross-check, we also computed the ggH amplitude and the decoupling constants through three loops using `MATAD` [29].

3 Calculation of decoupling constants

We aim for the calculation of all QCD decoupling constants up to four-loop order with general $SU(N_c)$ colour factors. They are obtained from ζ_3^0 , $\tilde{\zeta}_3^0$, ζ_2^0 and ζ_m^0 as introduced in Eq. (2) and the decoupling constant of the ghost-gluon vertex, $\tilde{\zeta}_1^0$. The decoupling constant for the gauge coupling is then given by

$$\zeta_g^0 = \frac{\tilde{\zeta}_1^0}{\tilde{\zeta}_3^0 \sqrt{\zeta_3^0}}. \quad (11)$$

The remaining decoupling constants for the gluon-quark vertex (ζ_1^0), the three-gluon vertex (ζ_{3g}^0) and four-gluon-vertex (ζ_{4g}^0) are obtained with the help of the Ward identities

$$\begin{aligned} \zeta_1^0 &= \zeta_g^0 \zeta_2^0 \sqrt{\zeta_3^0}, \\ \zeta_{3g}^0 &= \zeta_g^0 (\zeta_3^0)^{3/2}, \\ \zeta_{4g}^0 &= (\zeta_g^0)^2 (\zeta_3^0)^2. \end{aligned} \quad (12)$$

The bare decoupling constants ζ_3^0 , $\tilde{\zeta}_3^0$, ζ_2^0 and ζ_m^0 are obtained from the hard part of the gluon and ghost vacuum polarizations $\Pi_G(p^2)$ and $\Pi_c(p^2)$, as well as the vector and scalar parts of the light quark self-energy $\Sigma_V(p^2)$ and $\Sigma_S(p^2)$ as [1]

$$\begin{aligned} \zeta_3^0 &= 1 + \Pi_G^{0,h}(0), \\ \tilde{\zeta}_3^0 &= 1 + \Pi_c^{0,h}(0), \\ \zeta_2^0 &= 1 + \Sigma_V^{0,h}(0), \\ \zeta_m^0 &= \frac{1 - \Sigma_S^{0,h}(0)}{1 + \Sigma_V^{0,h}(0)}. \end{aligned} \quad (13)$$

To obtain the decoupling constants we only need the leading term in the limit $m_h \rightarrow \infty$. Thus, we can Taylor-expand in the external momenta and set them to zero after factoring out the tree-level tensor structure. This reduces the integrals to single-scale tadpole integrals. In analogy to Eq. (13), $\tilde{\zeta}_1^0$ is obtained from the ghost-gluon vertex

$$\tilde{\zeta}_1^0 = 1 + \Gamma_{G\bar{c}c}(p, q) \Big|_{p, q \rightarrow 0}. \quad (14)$$

where p and q are the four-momenta of the ghost and gluon, respectively. After projecting out the tree-level contribution both p and q are set to zero.

In Tab. 1 we present the number of diagrams generated by `qgraf` for the individual Green functions. Sample four-loop Feynman diagrams are shown in Fig. 1.

We perform the calculation keeping the full dependence on the gauge parameter ξ which drops out for $\zeta_{\alpha_s}^0$ and ζ_m^0 , as expected on general grounds. All other decoupling constants

# loops	1	2	3	4
$\Pi_G^{0,h}$	1	7	189	6 245
$\Pi_c^{0,h}$	—	1	25	765
$\Sigma_{V/S}^{0,h}$	—	1	25	765
$\Gamma_{G\bar{c}c}$	—	5	228	10 118

Table 1: Number of diagrams needed for computing the decoupling constants up to four loops.

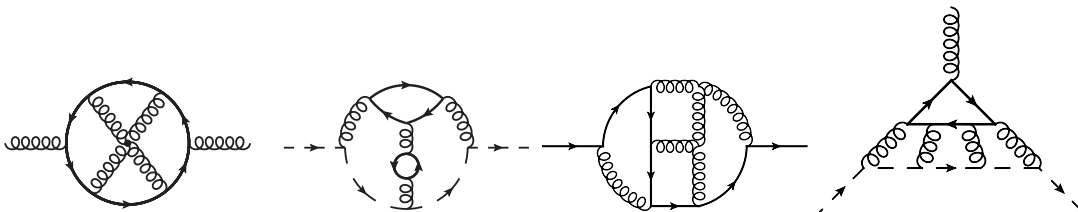


Figure 1: Sample four-loop diagrams contributing to the decoupling constants defined in Eqs. (13) and (14). Solid, curly and dashed lines refer to fermions, gluons and ghosts, respectively.

have an explicit ξ dependence. At three-loop order our results agree with those of Ref. [1] and at four loops we reproduce the results for ζ_{α_s} from Refs. [30, 31] and ζ_m from [32] after specifying $N_c = 3$.

The decoupling constants ζ_{α_s} and ζ_m as well as the leading terms of the others can be found in Appendix A. We provide the results for all renormalized decoupling constants in computer readable form in the ancillary files [33]. For convenience we offer several options concerning the renormalization scheme of the heavy quark ($\overline{\text{MS}}$ vs. on-shell) and α_s (n_f vs. n_l active flavours).

4 Direct calculation of matching coefficients

This section is devoted to the direct calculation of C_H and C_{HH} defined in the effective Lagrange density in Eq. (5). Two-loop results for C_H are known since the beginning of the eighties [34, 35] and at three-loop order C_H has been obtained for the first time from a direct calculation of the Higgs-gluon vertex in the large- m_t limit in Ref. [36] (see also Ref. [37]). Later the result has been confirmed with the help of a LET derived in Ref. [36] (see also Ref. [38]). Using the three-loop decoupling constant for α_s , the LET in combination with the four-loop beta function [9, 10] even leads to the four-loop result for C_H . The same reasoning has been applied in Refs. [30, 31, 39] to obtain the five-loop prediction for C_H , where an important input is provided by (the fermionic part of) the

# loops	1	2	3	4
ggH	2	23	657	23 251
$ggHH$ 1PI	6	99	3 192	124 149
$ggHH$ 1PR	—	8	216	7 200

Table 2: Number of diagrams needed for computing the Higgs-gluon amplitudes up to four loops.

five-loop beta function which has been computed in Refs. [40–42]. To date there is no direct calculation of C_H at four loops.

For C_{HH} the situation is as follows: at one- and two-loop order C_{HH} and C_H agree. At three-loop order a direct calculation has been performed in Ref. [15] by matching the full to the effective theory in Eq. (5). The result has been confirmed via the LET from Ref. [14], which can be used to derive the four-loop result for C_{HH} . It is one of the main aims of this paper to perform a direct calculation of C_{HH} and to confront it with the LET result.

In the following we use the notation for the matching equations introduced in Ref. [15]. We compute the ggH and $ggHH$ amplitudes in the limit where both the effective and the full theory are valid, i.e. for small external momenta as compared to the top quark mass. This leads again to single-scale vacuum integrals up to four-loop order. In the following we use $\alpha_s \equiv \alpha_s^{(5)}(\mu)$ if not indicated differently.

4.1 C_H

The Wilson coefficient is obtained by comparing the ggH amplitude in the effective and full theory which leads to the following matching formula

$$C_H Z_{\mathcal{O}_1} \mathcal{A}_{\text{LO}}^{\text{eff}} = \frac{1}{\zeta_3^0} \mathcal{A}^h + \mathcal{O}(1/m_t). \quad (15)$$

On the full-theory side \mathcal{A}^h denotes the hard part of the amplitude, which is obtained from a Taylor expansion in the two external momenta. It is assumed that the top quark mass and α_s are renormalized using standard counterterms up to three loops and the factor $1/\zeta_3^0$ takes care of the non-vanishing part of the gluon wave function renormalization. Due to our choice of the kinematic variables there are only tree-level contributions on the effective-theory side. Furthermore, we have the renormalization constant of the effective operator, $Z_{\mathcal{O}_1}$, and the sought-after (renormalized) matching coefficient C_H , which is obtained by dividing Eq. (15) by $Z_{\mathcal{O}_1}$. Note that $Z_{\mathcal{O}_1}$ depends on $\alpha_s^{(5)}$ whereas the quantities on the r.h.s. depend on $\alpha_s^{(6)}$. Before combining the various parts we use the decoupling constant to transform the strong coupling constant to $\alpha_s^{(5)}$. We renormalize the top quark mass in a first step in the $\overline{\text{MS}}$ scheme and transform to the on-shell scheme afterwards.

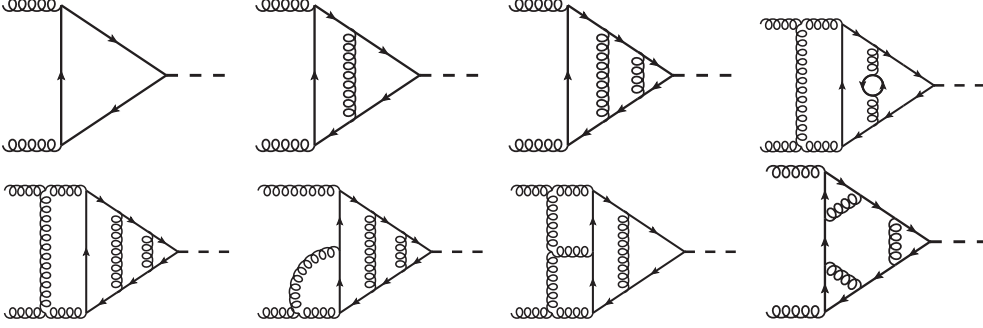


Figure 2: Sample one-, two-, three- and four-loop diagrams contributing to the $gg \rightarrow H$ amplitude. Solid and curly lines refer to fermions and gluons, respectively. The external Higgs boson is represented by a dashed line.

The number of diagrams generated by `qgraf` for \mathcal{A}^h is shown in Tab. 2 and sample Feynman diagrams are shown in Fig. 2. In a first step we apply the projector

$$P^{\mu\nu} = \frac{1}{2-2\epsilon} (g^{\mu\nu} q_1 \cdot q_2 - q_1^\nu q_2^\mu - q_1^\mu q_2^\nu) , \quad (16)$$

where q_1^μ and q_2^ν are the incoming four-momenta of the external gluons with polarization vectors $\varepsilon^\mu(q_1)$ and $\varepsilon^\nu(q_2)$. After tensor reduction we obtain the same kind of integral families as for the decoupling constants of the previous section.

As before, we perform the calculation for generic $SU(N_c)$ colour factors and full dependence on the gauge parameter ξ , which drops out after summing all contributions to \mathcal{A}^h . We cast the final result for the Wilson coefficient C_H in the form

$$C_H = -\frac{2\alpha_s T_F}{3\pi} \sum_{i=1} C_H^{(i)} \left(\frac{\alpha_s}{\pi}\right)^{(i-1)} , \quad (17)$$

where the $C^{(i)}$ are given by

$$C_H^{(1)} = 1 , \quad (18)$$

$$C_H^{(2)} = \frac{5}{4}C_A - \frac{3}{4}C_F , \quad (19)$$

$$C_H^{(3)} = \frac{1063}{576}C_A^2 - \frac{25}{12}C_A C_F - \frac{5}{96}C_A T_F + \frac{27}{32}C_F^2 - \frac{1}{12}C_F T_F \\ + \left[\frac{7}{16}C_A^2 - \frac{11}{16}C_A C_F \right] \ln\left(\frac{\mu^2}{M_t^2}\right) + n_t T_F \left[-\frac{47}{144}C_A - \frac{5}{16}C_F + \frac{1}{2}C_F \ln\left(\frac{\mu^2}{M_t^2}\right) \right] , \quad (20)$$

$$C_H^{(4)} = C_A^3 \left(\frac{110041}{41472} - \frac{1577}{3072}\zeta(3) \right) + C_A^2 C_F \left(-\frac{99715}{6912} + \frac{5105}{512}\zeta(3) \right) \\ + C_A^2 T_F \left(-\frac{1081}{3456} + \frac{1}{384}\zeta(3) \right) + C_A C_F^2 \left(\frac{2963}{384} - \frac{407}{128}\zeta(3) \right)$$

$$\begin{aligned}
& + C_A C_F T_F \left(\frac{4537}{1728} - \frac{115}{64} \zeta(3) \right) + C_A T_F^2 \left(\frac{2}{27} - \frac{7}{64} \zeta(3) \right) - \frac{471}{128} C_F^3 \\
& + C_F^2 T_F \left(-\frac{5}{12} + \frac{13}{32} \zeta(3) \right) + C_F T_F^2 \left(\frac{113}{432} - \frac{7}{32} \zeta(3) \right) \\
& + \frac{d_R^{abcd} d_A^{abcd}}{N_A T_F} \left(-\frac{2}{3} + \frac{13}{2} \zeta(3) \right) + \frac{d_R^{abcd} d_R^{abcd}}{N_A T_F} \left(\frac{11}{12} - 2\zeta(3) \right) \\
& + \left[\frac{1993}{1152} C_A^3 - \frac{275}{72} C_A^2 C_F - \frac{55}{576} C_A^2 T_F + \frac{99}{64} C_A C_F^2 - \frac{11}{72} C_A C_F T_F \right] \ln \left(\frac{\mu^2}{M_t^2} \right) \\
& + \left[\frac{77}{192} C_A^3 - \frac{121}{192} C_A^2 C_F \right] \ln^2 \left(\frac{\mu^2}{M_t^2} \right) + n_l \frac{d_R^{abcd} d_R^{abcd}}{N_A T_F} \left(\frac{11}{6} - 4\zeta(3) \right) \\
& + n_l T_F \left[C_A^2 \left(-\frac{12421}{10368} - \frac{151}{256} \zeta(3) \right) + C_A C_F \left(\frac{9605}{2592} - \frac{1145}{384} \zeta(3) \right) \right. \\
& \left. + C_A T_F \left(\frac{7}{216} - \frac{7}{64} \zeta(3) \right) + C_F^2 \left(\frac{215}{288} + \frac{127}{96} \zeta(3) \right) + C_F T_F \left(-\frac{29}{144} - \frac{7}{32} \zeta(3) \right) \right] \\
& + n_l^2 T_F^2 \left[-\frac{161}{2592} C_A - \frac{677}{1296} C_F \right] \\
& + n_l T_F \left[-\frac{55}{288} C_A^2 + \frac{55}{36} C_A C_F + \frac{5}{144} C_A T_F - \frac{5}{8} C_F^2 + \frac{1}{18} C_F T_F \right] \ln \left(\frac{\mu^2}{M_t^2} \right) \\
& + n_l^2 T_F^2 \left[\frac{5}{144} C_A + \frac{1}{18} C_F \right] \ln \left(\frac{\mu^2}{M_t^2} \right) + n_l T_F \left[-\frac{7}{48} C_A^2 + \frac{11}{16} C_A C_F \right] \ln^2 \left(\frac{\mu^2}{M_t^2} \right) \\
& - \frac{1}{6} n_l^2 C_F T_F^2 \ln^2 \left(\frac{\mu^2}{M_t^2} \right). \tag{21}
\end{aligned}$$

$\zeta(n)$ is the Riemann ζ -function, evaluated at n , M_t is the on-shell top quark mass and the $SU(N_c)$ colour factors are given by

$$\begin{aligned}
C_A = N_c, \quad C_F = \frac{N_c^2 - 1}{2N_c}, \quad T_F = \frac{1}{2}, \\
\frac{d_R^{abcd} d_A^{abcd}}{N_A} = \frac{N_c(N_c^2 + 6)}{48}, \quad \frac{d_R^{abcd} d_R^{abcd}}{N_A} = \frac{N_c^4 - 6N_c^2 + 18}{96N_c^2}, \tag{22}
\end{aligned}$$

with $N_A = N_c^2 - 1$. Note that C_H only contains $\zeta(3)$ as a transcendental constant while \mathcal{A}^h also contains other zeta-values and polylogarithms up to weight four. They cancel in the combination with $1/\zeta_3^0$ and only $\zeta(3)$ survives. After specifying $N_c = 3$ our result is in full agreement with the expression obtained with the help of the LET [1]. The latter can be used to obtain the five-loop result with full colour structure. We refrain from showing explicit results in the paper but include them in the ancillary files [33]. Let us remark that the five-loop result contains zeta-values and polylogarithms up to weight five.

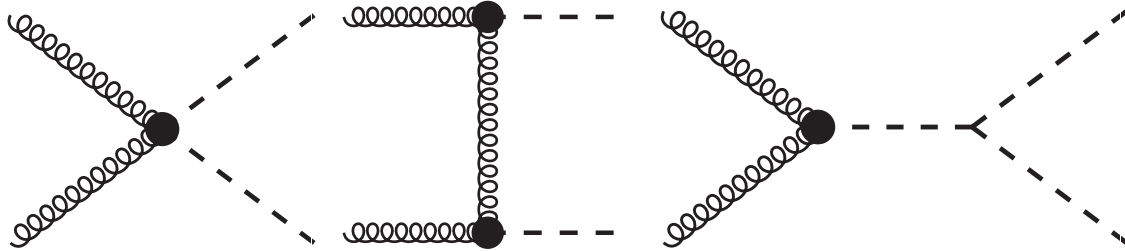


Figure 3: Tree-level contributions to the $gg \rightarrow HH$ amplitude in the effective theory. The blob indicates the insertion of the operator \mathcal{O}_1 . The left diagram is proportional to C_{HH} , the one in the middle to C_H^2 and the right diagram, which contains the trilinear Higgs coupling λ , to C_H . The amplitudes corresponding to the three Feynman diagrams are denoted by $\mathcal{A}_{\text{LO,1PI}}^{\text{eff}}$, $\mathcal{A}_{\text{LO,1PR},\lambda=0}^{\text{eff}}$ and $\mathcal{A}_{\text{LO,1PR},\lambda\neq 0}^{\text{eff}}$.

4.2 C_{HH}

The matching procedure to obtain C_{HH} is more involved as for C_H . First of all there are three contributions on the effective-theory side which are shown in Fig. 3: a one-particle irreducible (1PI) term proportional to C_{HH} , a one-particle reducible (1PR) term, which involves C_H^2 , and a term mediated by a virtual Higgs boson which splits into a Higgs boson pair via the Higgs boson self-coupling λ . The latter is similar in nature to the effective amplitude in the matching formula for C_H . In fact, also on the full-theory side this contribution involves diagrams which we already encountered in the computation of C_H . As mentioned in Ref. [15] it is easy to see, that these diagrams exactly cancel between the full and effective theory. Thus, the contributions relevant to extract C_{HH} are the 1PI and 1PR contribution with $\lambda = 0$.

The effective-theory side of the matching formula is obtained after renormalizing the operators in the various contributions of Fig. 3. Whereas the left and right contributions are both renormalized with a factor $Z_{\mathcal{O}_1}$, the term in the middle needs special care. In fact, a naive renormalization with $(Z_{\mathcal{O}_1})^2$ leads to uncanceled poles as has already been observed in Refs. [43, 44]. A careful analysis of the renormalization of the product of two operators \mathcal{O}_1 has been performed in Ref. [13] along the lines of [12]. It has been observed that apart from the naive multiplicative renormalization a further term is needed which is proportional to a single \mathcal{O}_1 . Adapting the findings of Ref. [13] to our notation one has

$$\mathcal{A}_{(\mathcal{O}_1)^2}^{\text{eff}} = Z_{\mathcal{O}_1}^2 \mathcal{A}_{(\mathcal{O}_1^0)^2}^{\text{eff}} + Z_{11}^L \mathcal{A}_{\mathcal{O}_1^0}^{\text{eff}} \quad (23)$$

where $\mathcal{A}_{\mathcal{O}_1^0}^{\text{eff}}$ and $\mathcal{A}_{(\mathcal{O}_1^0)^2}^{\text{eff}}$ correspond to amplitudes with one and two operator insertions. The renormalization constant Z_{11}^L (where L stands for ‘‘linear’’) is given by [13]

$$Z_{11}^L = \frac{1}{\epsilon} \left(1 - \frac{\beta(\alpha_s)}{\epsilon} \right)^{-2} \alpha_s^2 \frac{\partial}{\partial \alpha_s} \left[\frac{\beta(\alpha_s)}{\alpha_s} \right]. \quad (24)$$

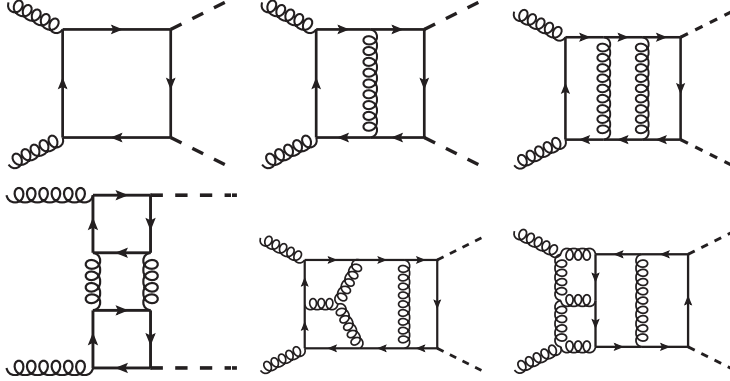


Figure 4: Sample one-, two-, three- and four-loop diagrams contributing $\mathcal{A}_{1\text{PI}}^h$ in Eq. (26).

It has its first non-vanishing contribution at order α_s^2 . As we will see below, in our calculation we need the combination $Z_{11}^L/Z_{\mathcal{O}_1}$ up to order α_s^2 which is given by

$$\frac{Z_{11}^L}{Z_{\mathcal{O}_1}} = -\frac{\beta_1}{\epsilon} \frac{\alpha_s^2}{(4\pi)^2} + \mathcal{O}(\alpha_s^3). \quad (25)$$

We are now in the position to write down the matching formula for C_{HH} . Complementing the effective-theory side, which is basically given by Fig. 3, with the corresponding full-theory amplitudes and taking into account Eq. (23) leads to²

$$\begin{aligned} & (C_{HH}Z_{\mathcal{O}_1} + C_H^2Z_{11}^L)\mathcal{A}_{\text{LO},1\text{PI}}^{\text{eff}} + C_H^2Z_{\mathcal{O}_1}^2\mathcal{A}_{\text{LO},1\text{PR},\lambda=0}^{\text{eff}} + C_HZ_{\mathcal{O}_1}\mathcal{A}_{\text{LO},1\text{PR},\lambda\neq 0}^{\text{eff}} \\ &= \frac{1}{\zeta_0^3} (\mathcal{A}_{1\text{PI}}^h + \mathcal{A}_{1\text{PR},\lambda=0}^h + \mathcal{A}_{1\text{PR},\lambda\neq 0}^h) + \mathcal{O}(1/m_t), \end{aligned} \quad (26)$$

where sample Feynman diagrams contributing to $\mathcal{A}_{1\text{PI}}^h$ and $\mathcal{A}_{1\text{PR},\lambda=0}^h$ can be found in Figs. 4 and 5, respectively. As already mentioned above, the contributions with $\lambda \neq 0$ cancel in Eq. (26). Note that our matching formula differs from the one of Ref. [15] by the term proportional to Z_{11}^L which contributes for the first time at four-loop order, since both C_H^2 and Z_{11}^L are of order α_s^2 .

Let us in the following discuss some features of the matching procedure. At one-loop order the only non-zero contribution on the r.h.s. of Eq. (26) is $\mathcal{A}_{1\text{PI}}^h$ and one obtains $C_{HH}^{(1)} = C_H^{(1)}$. This also holds at two-loops where the 1PR contributions on effective- and full-theory side match exactly. A non-trivial interplay between $\mathcal{A}_{1\text{PI}}^h$ and $\mathcal{A}_{1\text{PR},\lambda=0}^h$ is observed for the first time at three-loop order [15]. In fact the 1PI and 1PR contributions are not separately finite any more and the poles only cancel in the sum. Starting from this order C_{HH} is different from C_H . While the 1PI and 1PR contributions are separately

²When applying Eq. (23) to Higgs boson pair production we have $\mathcal{A}_{(\mathcal{O}_1)^2}^{\text{eff}} = \mathcal{A}_{\text{LO},1\text{PR},\lambda=0}^{\text{eff}}$ and $\mathcal{A}_{\mathcal{O}_1^0}^{\text{eff}} = \mathcal{A}_{\text{LO},1\text{PI}}^{\text{eff}}$.

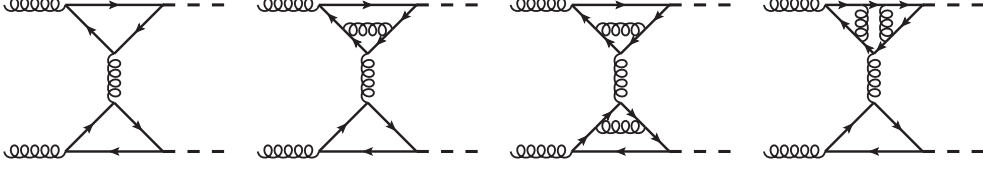


Figure 5: Sample two-, three- and four-loop diagrams contributing to $\mathcal{A}_{1\text{PR},\lambda=0}^h$ in Eq. (26).

ξ -independent at three loops, for the four-loop colour structure $C_A^2 T_F$ it only drops out in the proper combination.

We computed the 1PI and 1PR amplitudes in the full theory separately and keep in both cases terms linear in the gauge parameter ξ . For both contributions it is important to keep the three external momenta different from zero and different from each other in order to avoid the mixing with unphysical operators [12]. The external momenta can be set to zero after projection to the matching coefficient which is done with the help of

$$P^{\mu\nu} = \frac{1}{2 - 4\epsilon} \left(\frac{q_1^\nu q_2^\mu q_{33}}{2q_{12}q_T^2} - \frac{q_1^\nu q_2^\mu}{2q_{12}} - \frac{q_1^\nu q_3^\mu q_{23}}{q_{12}q_T^2} - \frac{q_2^\mu q_3^\nu q_{13}}{q_{12}q_T^2} + \frac{q_3^\mu q_3^\nu}{q_T^2} + g^{\mu\nu} \right) - \frac{q_1^\nu q_2^\mu q_{33}}{4q_{12}q_T^2} - \frac{q_1^\nu q_2^\mu}{4q_{12}} + \frac{q_1^\nu q_3^\mu q_{23}}{2q_{12}q_T^2} + \frac{q_2^\mu q_3^\nu q_{13}}{2q_{12}q_T^2} - \frac{q_3^\mu q_3^\nu}{2q_T^2}, \quad (27)$$

where $q_{ij} = q_i \cdot q_j$ and $q_T^2 = 2q_{13}q_{23}/q_{12} - q_{33}$. q_1^μ and q_2^ν are the incoming four-momenta of the external gluons with polarization vectors $\varepsilon^\mu(q_1)$ and $\varepsilon^\nu(q_2)$ and q_3 is the incoming four-momentum of one of the Higgs bosons.

The number of diagrams for the 1PI amplitude can be found in Tab. 2 and sample diagrams are shown in Fig. 4. Once the projector of Eq. (27) is applied one obtains scalar expressions which still contain scalar products of q_1 , q_2 and q_3 and loop momenta in the numerator. After solving the corresponding tensor vacuum integrals the resulting scalar products q_{ij} cancel against the corresponding contributions with negative powers from the projector and all external momenta can be set to zero.

The 1PR amplitude has been obtained in two different ways. First, we computed the 1PR diagrams up to four-loop order (see Tab. 2 for the number of diagrams and Fig. 5 for typical Feynman diagrams) in analogy to the 1PI contribution. As a cross-check we computed the 1PI parts of the 1PR contributions separately and constructed the n -loop 1PR $ggHH$ amplitude from ggH amplitudes computed up to $(n - 1)$ loops. In this approach one of the gluons in the ggH amplitude has to be off-shell, which leads to more non-vanishing Lorentz structures. In practice, we computed the 1PI ggH amplitudes with open Lorentz indices up to three loops. Full agreement has been found between the two methods.

We cast the final result for the Wilson coefficient C_{HH} in the form

$$C_{HH} = -\frac{2\alpha_s}{3\pi} T_F \sum_{i=1} \left(C_H^{(i)} + \Delta_{HH}^{(i)} \right) \left(\frac{\alpha_s}{\pi} \right)^{(i-1)}, \quad (28)$$

where the $C_H^{(i)}$ are given in Eq. (21) and the differences are given by

$$\begin{aligned}
\Delta_{HH}^{(1)} &= 0, \\
\Delta_{HH}^{(2)} &= 0, \\
\Delta_{HH}^{(3)} &= \frac{7}{8}C_A^2 - \frac{11}{8}C_A C_F - \frac{5}{6}C_A T_F + \frac{1}{2}C_F T_F + n_l C_F T_F, \\
\Delta_{HH}^{(4)} &= \frac{1993}{576}C_A^3 - \frac{1289}{144}C_A^2 C_F - \frac{3191}{864}C_A^2 T_F + \frac{165}{32}C_A C_F^2 + \frac{67}{18}C_A C_F T_F + \frac{5}{72}C_A T_F^2 \\
&\quad - \frac{3}{2}C_F^2 T_F + \frac{1}{9}C_F T_F^2 + \left[\frac{77}{48}C_A^3 - \frac{121}{48}C_A^2 C_F - \frac{7}{12}C_A^2 T_F + \frac{11}{12}C_A C_F T_F \right] \ln \left(\frac{\mu^2}{M_t^2} \right) \\
&\quad + n_l T_F \left[-\frac{55}{144}C_A^2 + \frac{55}{18}C_A C_F + \frac{109}{216}C_A T_F - \frac{11}{4}C_F^2 + \frac{19}{36}C_F T_F \right] \\
&\quad + n_l^2 T_F^2 \left[\frac{5}{72}C_A + \frac{1}{9}C_F \right] + n_l T_F \left[-\frac{7}{12}C_A^2 + \frac{11}{4}C_A C_F - \frac{2}{3}C_F T_F \right] \ln \left(\frac{\mu^2}{M_t^2} \right) \\
&\quad - \frac{2}{3}n_l^2 C_F T_F^2 \ln \left(\frac{\mu^2}{M_t^2} \right). \tag{29}
\end{aligned}$$

The three-loop result can be found in Ref. [15]. Our four-loop result $\Delta_{HH}^{(4)}$ agrees with the expression from Eq. (10) [14]. We can thus confirm the validity of the LET for C_{HH} [14] through four loops. In analogy to C_H also for C_{HH} it is possible to construct the five-loop approximation for general colour structure. The corresponding results can be found in computer readable form in the ancillary files [33]. After specifying to $N_c = 3$ we agree with the numerical results given in Ref [14], both for $\overline{\text{MS}}$ and on-shell top quark mass.

5 Conclusions

We perform for the first time a direct four-loop computation of the Wilson coefficients C_H and C_{HH} of the effective operators, which couple gluons to one and two Higgs bosons, respectively. C_H and C_{HH} enter as building blocks various physical quantities, e.g., the next-to-next-to-next-to-leading order predictions for single [45,46] and double Higgs boson production.³ Our results for C_H and C_{HH} agree with the expression obtained by means of LETs. Furthermore, we compute all QCD decoupling constants up to four-loop order. If possible we compared with the literature and find agreement after specifying the colour factors. All our results are expressed for general $\text{SU}(N_c)$ colour factors whereas the four-loop expressions in the literature are only available for $N_c = 3$.

A major result of this paper is the derivation of the matching equation (26) which receives a non-trivial renormalization contribution from the effective-theory amplitude with two

³See also the recent paper [47] where two-loop massless four-point amplitudes have been computed, a further building block to next-to-next-to-next-to-leading order double Higgs boson production.

insertions of the operator \mathcal{O}_1 . The new term contributes for the first time at four-loop order and is essential to obtain a finite result.

For the convenience of the reader we collect all analytic results obtained in this paper in ancillary files [33].

Acknowledgements

We thank Kirill Melnikov and Konstantin Chetyrkin for fruitful discussions and Konstantin Chetyrkin for drawing our attention to Ref. [13]. F.H. acknowledges the support by the DFG-funded Doctoral School KSETA.

A Decoupling constants

In this appendix we collect the results for the decoupling constants for general $SU(N_c)$ colour factors. We provide results for ζ_{α_s} and ζ_m up to four loops and show for all other ζ s the expressions for the first non-vanishing loop-order. Computer readable expressions up to four loops can be found in [33]. Our results read

$$\zeta_X = 1 + \sum_{i=1} \zeta_X^{(i)} \left(\frac{\alpha_s^{(n_f)}}{\pi} \right)^i, \quad (30)$$

where

$$\begin{aligned} \zeta_{\alpha_s}^{(1)} &= -\frac{1}{3} T_F \ln \left(\frac{\mu^2}{m^2} \right), \\ \zeta_{\alpha_s}^{(2)} &= \frac{2}{9} C_A T_F - \frac{13}{48} C_F T_F + \left(-\frac{5}{12} C_A T_F + \frac{1}{4} C_F T_F \right) \ln \left(\frac{\mu^2}{m^2} \right) + \frac{1}{9} T_F^2 \ln^2 \left(\frac{\mu^2}{m^2} \right), \\ \zeta_{\alpha_s}^{(3)} &= C_A^2 T_F \left(\frac{11347}{20736} - \frac{5}{1536} \zeta(3) \right) + C_A C_F T_F \left(\frac{2999}{2592} - \frac{1273}{768} \zeta(3) \right) + C_A T_F^2 \left(\frac{245}{5184} \right. \\ &\quad \left. - \frac{7}{128} \zeta(3) \right) + C_F^2 T_F \left(-\frac{97}{288} + \frac{95}{192} \zeta(3) \right) + C_F T_F^2 \left(\frac{103}{1296} - \frac{7}{64} \zeta(3) \right) \\ &\quad + n_l T_F \left[-\frac{1}{2592} C_A T_F - \frac{41}{162} C_F T_F \right] + \left[-\frac{1063}{1728} C_A^2 T_F + \frac{25}{36} C_A C_F T_F - \frac{113}{864} C_A T_F^2 \right. \\ &\quad \left. - \frac{9}{32} C_F^2 T_F + \frac{5}{24} C_F T_F^2 \right] \ln \left(\frac{\mu^2}{m^2} \right) + \left[-\frac{7}{96} C_A^2 T_F + \frac{11}{96} C_A C_F T_F + \frac{25}{72} C_A T_F^2 \right. \\ &\quad \left. - \frac{5}{24} C_F T_F^2 \right] \ln^2 \left(\frac{\mu^2}{m^2} \right) - \frac{1}{27} T_F^3 \ln^3 \left(\frac{\mu^2}{m^2} \right) + n_l T_F \left[\frac{47}{432} C_A T_F + \frac{5}{48} C_F T_F \right] \ln \left(\frac{\mu^2}{m^2} \right) \end{aligned}$$

$$\begin{aligned}
& -\frac{1}{12}n_l C_F T_F^2 \ln^2\left(\frac{\mu^2}{m^2}\right), \\
\zeta_{\alpha_s}^{(4)} = & C_A^3 T_F \left(\frac{14060183}{13063680} - \frac{4663}{630} \text{Li}_5\left(\frac{1}{2}\right) + \frac{24153}{2240} \text{Li}_4\left(\frac{1}{2}\right) + \frac{8051}{17920} \ln^4(2) \right. \\
& + \frac{4663}{75600} \ln^5(2) + \frac{377777}{40320} \zeta(5) - \frac{6668653}{645120} \zeta(4) - \frac{70841}{10080} \zeta(4) \ln(2) + \frac{1331653}{215040} \zeta(3) \\
& - \frac{24153}{8960} \zeta(2) \ln^2(2) - \left. \frac{4663}{7560} \zeta(2) \ln^3(2) \right) + C_A^2 C_F T_F \left(\frac{69024559}{10450944} + \frac{8674}{315} \text{Li}_5\left(\frac{1}{2}\right) \right. \\
& - \frac{11}{105} \text{Li}_4\left(\frac{1}{2}\right) - \frac{11}{2520} \ln^4(2) - \frac{4337}{18900} \ln^5(2) - \frac{1411867}{40320} \zeta(5) + \frac{4919}{8960} \zeta(4) \\
& + \frac{280261}{10080} \zeta(4) \ln(2) - \frac{1639301}{193536} \zeta(3) + \frac{11}{420} \zeta(2) \ln^2(2) + \left. \frac{4337}{1890} \zeta(2) \ln^3(2) \right) \\
& + C_A^2 T_F^2 \left(-\frac{6301303}{65318400} - \frac{8099}{1440} \text{Li}_4\left(\frac{1}{2}\right) - \frac{8099}{34560} \ln^4(2) + \frac{5}{144} \zeta(5) + \frac{30103}{5120} \zeta(4) \right. \\
& - \frac{18564121}{4838400} \zeta(3) + \left. \frac{8099}{5760} \zeta(2) \ln^2(2) \right) + C_A C_F^2 T_F \left(-\frac{556181}{145152} - \frac{14458}{315} \text{Li}_5\left(\frac{1}{2}\right) \right. \\
& - \frac{39521}{560} \text{Li}_4\left(\frac{1}{2}\right) - \frac{39521}{13440} \ln^4(2) + \frac{7229}{18900} \ln^5(2) + \frac{1214657}{20160} \zeta(5) + \frac{3818767}{53760} \zeta(4) \\
& - \frac{13991}{315} \zeta(4) \ln(2) - \frac{1990813}{48384} \zeta(3) + \frac{39521}{2240} \zeta(2) \ln^2(2) - \left. \frac{7229}{1890} \zeta(2) \ln^3(2) \right) \\
& + C_A C_F T_F^2 \left(\frac{12072043}{8164800} + \frac{1457}{90} \text{Li}_4\left(\frac{1}{2}\right) + \frac{1457}{2160} \ln^4(2) - \frac{5}{24} \zeta(5) - \frac{24673}{1440} \zeta(4) \right. \\
& + \frac{8133593}{806400} \zeta(3) - \left. \frac{1457}{360} \zeta(2) \ln^2(2) \right) + C_A T_F^3 \left(\frac{6641}{1306368} - \frac{545}{18144} \zeta(3) \right) \\
& + C_F^3 T_F \left(\frac{37441}{34560} + \frac{256}{15} \text{Li}_5\left(\frac{1}{2}\right) + \frac{1919}{45} \text{Li}_4\left(\frac{1}{2}\right) + \frac{1919}{1080} \ln^4(2) - \frac{32}{225} \ln^5(2) \right. \\
& - \frac{3429}{160} \zeta(5) - \frac{58001}{1440} \zeta(4) + \frac{212}{15} \zeta(4) \ln(2) + \frac{7549}{320} \zeta(3) - \frac{1919}{180} \zeta(2) \ln^2(2) \\
& + \left. \frac{64}{45} \zeta(2) \ln^3(2) \right) + C_F^2 T_F^2 \left(\frac{2337647}{1036800} + \frac{874}{45} \text{Li}_4\left(\frac{1}{2}\right) + \frac{437}{540} \ln^4(2) - \frac{29737}{1440} \zeta(4) \right. \\
& + \frac{123149}{10800} \zeta(3) - \left. \frac{437}{90} \zeta(2) \ln^2(2) \right) + C_F T_F^3 \left(-\frac{610843}{3265920} + \frac{661}{3780} \zeta(3) \right) \\
& + \frac{d_R^{abcd} d_A^{abcd}}{N_A} \left(\frac{6617}{30240} + \frac{7496}{105} \text{Li}_5\left(\frac{1}{2}\right) + \frac{3988}{105} \text{Li}_4\left(\frac{1}{2}\right) + \frac{997}{630} \ln^4(2) - \frac{937}{1575} \ln^5(2) \right. \\
& - \frac{274067}{3360} \zeta(5) - \frac{194179}{6720} \zeta(4) + \frac{49661}{840} \zeta(4) \ln(2) + \frac{322631}{20160} \zeta(3) - \frac{997}{105} \zeta(2) \ln^2(2) \\
& + \left. \frac{1874}{315} \zeta(2) \ln^3(2) \right) + \frac{d_R^{abcd} d_R^{abcd}}{N_A} \left(-\frac{2411}{5040} + \frac{73}{6} \text{Li}_4\left(\frac{1}{2}\right) + \frac{73}{144} \ln^4(2) + \frac{5}{12} \zeta(5) \right. \\
& - \left. \frac{2189}{192} \zeta(4) + \frac{6779}{1120} \zeta(3) - \frac{73}{24} \zeta(2) \ln^2(2) \right)
\end{aligned}$$

$$\begin{aligned}
& + n_l \left[C_A^2 T_F^2 \left(-\frac{252017}{373248} - \frac{5}{16} \text{Li}_4 \left(\frac{1}{2} \right) - \frac{5}{384} \ln^4(2) + \frac{5}{72} \zeta(5) - \frac{59}{512} \zeta(4) \right. \right. \\
& + \frac{11813}{27648} \zeta(3) + \left. \frac{5}{64} \zeta(2) \ln^2(2) \right) + C_A C_F T_F^2 \left(-\frac{35455}{62208} + \frac{143}{72} \text{Li}_4 \left(\frac{1}{2} \right) + \frac{143}{1728} \ln^4(2) \right. \\
& - \frac{9359}{2304} \zeta(4) + \frac{45287}{13824} \zeta(3) - \left. \frac{143}{288} \zeta(2) \ln^2(2) \right) + C_A T_F^3 \left(\frac{4171}{62208} + \frac{1}{12} \text{Li}_4 \left(\frac{1}{2} \right) \right. \\
& + \frac{1}{288} \ln^4(2) - \frac{49}{384} \zeta(4) - \frac{59}{3456} \zeta(3) - \left. \frac{1}{48} \zeta(2) \ln^2(2) \right) + C_F^2 T_F^2 \left(-\frac{19}{324} - \frac{49}{18} \text{Li}_4 \left(\frac{1}{2} \right) \right. \\
& - \frac{49}{432} \ln^4(2) + \frac{1453}{576} \zeta(4) - \frac{1955}{1728} \zeta(3) + \left. \frac{49}{72} \zeta(2) \ln^2(2) \right) + C_F T_F^3 \left(-\frac{8663}{93312} \right. \\
& + \frac{1}{6} \text{Li}_4 \left(\frac{1}{2} \right) + \frac{1}{144} \ln^4(2) - \frac{49}{192} \zeta(4) + \frac{77}{432} \zeta(3) - \left. \frac{1}{24} \zeta(2) \ln^2(2) \right) \\
& + \left. \frac{d_R^{abcd} d_A^{abcd}}{N_A} \left(-\frac{103}{216} + \frac{5}{6} \zeta(5) + \frac{1}{2} \zeta(4) - \frac{131}{72} \zeta(3) \right) \right] \\
& + n_l^2 \left[C_A T_F^3 \left(-\frac{841}{62208} - \frac{5}{216} \zeta(3) \right) + C_F T_F^3 \left(-\frac{31147}{93312} + \frac{53}{216} \zeta(3) \right) \right] \\
& + \left[C_A^3 T_F \left(-\frac{110041}{124416} + \frac{1577}{9216} \zeta(3) \right) + C_A^2 C_F T_F \left(\frac{105763}{20736} - \frac{5105}{1536} \zeta(3) \right) \right. \\
& + C_A^2 T_F^2 \left(-\frac{2093}{3888} + \frac{1}{768} \zeta(3) \right) + C_A C_F^2 T_F \left(-\frac{3491}{1152} + \frac{407}{384} \zeta(3) \right) + C_A C_F T_F^2 \left(-\frac{8875}{7776} \right. \\
& + \left. \frac{1963}{1152} \zeta(3) \right) + C_A T_F^3 \left(-\frac{437}{7776} + \frac{7}{96} \zeta(3) \right) + \frac{157}{128} C_F^3 T_F + C_F^2 T_F^2 \left(+\frac{277}{1728} - \frac{67}{144} \zeta(3) \right) \\
& + C_F T_F^3 \left(-\frac{545}{3888} + \frac{7}{48} \zeta(3) \right) + \left. \frac{d_R^{abcd} d_A^{abcd}}{N_A} \left(\frac{2}{9} - \frac{13}{6} \zeta(3) \right) \right] \\
& + \frac{d_R^{abcd} d_R^{abcd}}{N_A} \left(-\frac{11}{36} + \frac{2}{3} \zeta(3) \right) \ln \left(\frac{\mu^2}{m^2} \right) + \left[-\frac{1993}{6912} C_A^3 T_F + \frac{1289}{1728} C_A^2 C_F T_F \right. \\
& + \frac{1027}{1152} C_A^2 T_F^2 - \frac{55}{128} C_A C_F^2 T_F - \frac{53}{54} C_A C_F T_F^2 + \frac{49}{864} C_A T_F^3 + \frac{3}{8} C_F^2 T_F^2 \\
& - \left. \frac{17}{144} C_F T_F^3 \right] \ln^2 \left(\frac{\mu^2}{m^2} \right) + \left[-\frac{77}{1728} C_A^3 T_F + \frac{121}{1728} C_A^2 C_F T_F + \frac{35}{432} C_A^2 T_F^2 \right. \\
& - \left. \frac{55}{432} C_A C_F T_F^2 - \frac{65}{324} C_A T_F^3 + \frac{13}{108} C_F T_F^3 \right] \ln^3 \left(\frac{\mu^2}{m^2} \right) + \frac{1}{81} T_F^4 \ln^4 \left(\frac{\mu^2}{m^2} \right) \\
& + n_l \left[C_A^2 T_F^2 \left(\frac{12421}{31104} + \frac{151}{768} \zeta(3) \right) + C_A C_F T_F^2 \left(-\frac{9605}{7776} + \frac{1145}{1152} \zeta(3) \right) + C_A T_F^3 \left(-\frac{41}{3888} \right. \right. \\
& + \left. \frac{7}{192} \zeta(3) \right) + C_F^2 T_F^2 \left(\frac{73}{864} - \frac{127}{288} \zeta(3) \right) + C_F T_F^3 \left(\frac{917}{3888} + \frac{7}{96} \zeta(3) \right) + \left. \frac{d_R^{abcd} d_R^{abcd}}{N_A} \left(-\frac{11}{18} \right. \right.
\end{aligned}$$

$$\begin{aligned}
& + \frac{4}{3}\zeta(3) \left] \ln\left(\frac{\mu^2}{m^2}\right) + n_l^2 \left[\frac{161}{7776}C_A T_F^3 + \frac{677}{3888}C_F T_F^3 \right] \ln\left(\frac{\mu^2}{m^2}\right) + n_l \left[\frac{55}{1728}C_A^2 T_F^2 \right. \\
& - \frac{55}{216}C_A C_F T_F^2 - \frac{11}{96}C_A T_F^3 + \frac{11}{48}C_F^2 T_F^2 - \frac{49}{432}C_F T_F^3 \left. \right] \ln^2\left(\frac{\mu^2}{m^2}\right) + n_l^2 \left[-\frac{5}{864}C_A T_F^3 \right. \\
& - \frac{1}{108}C_F T_F^3 \left. \right] \ln^2\left(\frac{\mu^2}{m^2}\right) + n_l \left[\frac{7}{432}C_A^2 T_F^2 - \frac{11}{144}C_A C_F T_F^2 + \frac{5}{54}C_F T_F^3 \right] \ln^3\left(\frac{\mu^2}{m^2}\right) \\
& + \frac{1}{54}n_l^2 C_F T_F^3 \ln^3\left(\frac{\mu^2}{m^2}\right) , \tag{31}
\end{aligned}$$

$$\zeta_m^{(1)} = 0 ,$$

$$\zeta_m^{(2)} = \frac{89}{288}C_F T_F - \frac{5}{24}C_F T_F \ln\left(\frac{\mu^2}{m^2}\right) + \frac{1}{8}C_F T_F \ln^2\left(\frac{\mu^2}{m^2}\right) ,$$

$$\begin{aligned}
\zeta_m^{(3)} &= C_A C_F T_F \left(\frac{16627}{15552} - 2\text{Li}_4\left(\frac{1}{2}\right) - \frac{1}{12}\ln^4(2) + \frac{31}{16}\zeta(4) - \frac{629}{576}\zeta(3) + \frac{1}{2}\zeta(2)\ln^2(2) \right) \\
&+ C_F^2 T_F \left(-\frac{683}{576} + 4\text{Li}_4\left(\frac{1}{2}\right) + \frac{1}{6}\ln^4(2) - \frac{11}{4}\zeta(4) + \frac{57}{32}\zeta(3) - \zeta(2)\ln^2(2) \right) \\
&+ C_F T_F^2 \left(-\frac{1685}{7776} + \frac{7}{18}\zeta(3) \right) + n_l C_F T_F^2 \left(\frac{1327}{3888} - \frac{2}{9}\zeta(3) \right) + \left[C_A C_F T_F \left(\frac{5}{64} - \frac{3}{4}\zeta(3) \right) \right. \\
&+ C_F^2 T_F \left(-\frac{13}{64} + \frac{3}{4}\zeta(3) \right) - \frac{31}{108}C_F T_F^2 \left. \right] \ln\left(\frac{\mu^2}{m^2}\right) + \left[\frac{29}{96}C_A C_F T_F - \frac{1}{4}C_F^2 T_F \right. \\
&+ \frac{5}{72}C_F T_F^2 \left. \right] \ln^2\left(\frac{\mu^2}{m^2}\right) + \left[\frac{11}{144}C_A C_F T_F - \frac{1}{18}C_F T_F^2 \right] \ln^3\left(\frac{\mu^2}{m^2}\right) \\
&- \frac{53}{144}n_l C_F T_F^2 \ln\left(\frac{\mu^2}{m^2}\right) - \frac{1}{36}n_l C_F T_F^2 \ln^3\left(\frac{\mu^2}{m^2}\right) ,
\end{aligned}$$

$$\begin{aligned}
\zeta_m^{(4)} &= C_A^2 C_F T_F \left(\frac{4524863}{829440} - \frac{173}{15}\text{Li}_5\left(\frac{1}{2}\right) - \frac{14539}{640}\text{Li}_4\left(\frac{1}{2}\right) - \frac{14539}{15360}\ln^4(2) + \frac{173}{1800}\ln^5(2) \right. \\
&- \frac{5}{32}\zeta(6) + \frac{7551}{1280}\zeta(5) + \frac{759689}{30720}\zeta(4) - \frac{1883}{120}\zeta(4)\ln(2) - \frac{1640279}{184320}\zeta(3) - \frac{21}{128}\zeta(3)^2 \\
&+ \frac{14539}{2560}\zeta(2)\ln^2(2) - \frac{173}{180}\zeta(2)\ln^3(2) \left. \right) + C_A C_F^2 T_F \left(\frac{1068103}{414720} + \frac{514}{15}\text{Li}_5\left(\frac{1}{2}\right) \right. \\
&+ \frac{11321}{320}\text{Li}_4\left(\frac{1}{2}\right) + \frac{11321}{7680}\ln^4(2) - \frac{257}{900}\ln^5(2) - \frac{425}{128}\zeta(6) - \frac{77977}{1920}\zeta(5) - \frac{181317}{5120}\zeta(4) \\
&+ \frac{1321}{30}\zeta(4)\ln(2) + \frac{398489}{30720}\zeta(3) - \frac{11}{32}\zeta(3)^2 - \frac{11321}{1280}\zeta(2)\ln^2(2) + \frac{257}{90}\zeta(2)\ln^3(2) \left. \right) \\
&+ C_A C_F T_F^2 \left(-\frac{214882117}{203212800} + \frac{28657}{3360}\text{Li}_4\left(\frac{1}{2}\right) + \frac{28657}{80640}\ln^4(2) + \frac{97}{24}\zeta(5) - \frac{152979}{17920}\zeta(4) \right)
\end{aligned}$$

$$\begin{aligned}
& + \frac{29927237}{11289600} \zeta(3) - \frac{28657}{13440} \zeta(2) \ln^2(2) \Big) + C_F^3 T_F \left(\frac{10301}{10240} - \frac{112}{5} \text{Li}_5 \left(\frac{1}{2} \right) + \frac{3227}{240} \text{Li}_4 \left(\frac{1}{2} \right) \right. \\
& + \frac{3227}{5760} \ln^4(2) + \frac{14}{75} \ln^5(2) + \frac{65}{64} \zeta(6) + \frac{10003}{320} \zeta(5) - \frac{20897}{1920} \zeta(4) - \frac{253}{10} \zeta(4) \ln(2) \\
& + \frac{1427}{480} \zeta(3) + \frac{87}{32} \zeta(3)^2 - \frac{3227}{960} \zeta(2) \ln^2(2) - \frac{28}{15} \zeta(2) \ln^3(2) \Big) + C_F^2 T_F^2 \left(\frac{257128337}{203212800} \right. \\
& + \frac{5041}{1680} \text{Li}_4 \left(\frac{1}{2} \right) + \frac{5041}{40320} \ln^4(2) - \frac{63}{16} \zeta(5) - \frac{90269}{26880} \zeta(4) + \frac{7671973}{1881600} \zeta(3) \\
& - \frac{5041}{6720} \zeta(2) \ln^2(2) \Big) + C_F T_F^3 \left(\frac{1281821}{19595520} + \frac{1}{48} \zeta(4) + \frac{51}{560} \zeta(3) \right) + \frac{d_R^{abcd} d_R^{abcd}}{N_F} \left(-\frac{611}{384} \right. \\
& + 40 \text{Li}_4 \left(\frac{1}{2} \right) + \frac{5}{3} \ln^4(2) - \frac{15}{4} \zeta(6) - \frac{135}{32} \zeta(5) - \frac{1445}{64} \zeta(4) + \frac{973}{64} \zeta(3) + \frac{15}{4} \zeta(3)^2 \\
& - 10 \zeta(2) \ln^2(2) \Big) + n_l \left[C_A C_F T_F^2 \left(-\frac{5095}{3072} + 4 \text{Li}_5 \left(\frac{1}{2} \right) + \frac{49}{12} \text{Li}_4 \left(\frac{1}{2} \right) + \frac{49}{288} \ln^4(2) \right. \right. \\
& - \frac{1}{30} \ln^5(2) - \frac{253}{96} \zeta(5) - \frac{543}{128} \zeta(4) + \frac{49}{8} \zeta(4) \ln(2) - \frac{65}{192} \zeta(3) - \frac{49}{48} \zeta(2) \ln^2(2) \\
& + \frac{1}{3} \zeta(2) \ln^3(2) \Big) + C_F^2 T_F^2 \left(-\frac{15557}{5184} - 8 \text{Li}_5 \left(\frac{1}{2} \right) - \frac{49}{6} \text{Li}_4 \left(\frac{1}{2} \right) - \frac{49}{144} \ln^4(2) \right. \\
& + \frac{1}{15} \ln^5(2) + \frac{157}{16} \zeta(5) + \frac{1639}{192} \zeta(4) - \frac{49}{4} \zeta(4) \ln(2) - \frac{5}{8} \zeta(3) + \frac{49}{24} \zeta(2) \ln^2(2) \\
& - \frac{2}{3} \zeta(2) \ln^3(2) \Big) + C_F T_F^3 \left(-\frac{57}{256} + \frac{9}{16} \zeta(4) - \frac{5}{144} \zeta(3) \right) \Big] + n_i^2 C_F T_F^3 \left(\frac{17671}{20736} - \frac{7}{16} \zeta(4) \right. \\
& - \frac{5}{144} \zeta(3) \Big) + \left[C_A^2 C_F T_F \left(\frac{233903}{248832} - \frac{11}{2} \text{Li}_4 \left(\frac{1}{2} \right) - \frac{11}{48} \ln^4(2) + \frac{25}{16} \zeta(5) + \frac{407}{64} \zeta(4) \right. \right. \\
& - \frac{119723}{18432} \zeta(3) + \frac{11}{8} \zeta(2) \ln^2(2) \Big) + C_A C_F^2 T_F \left(-\frac{3529}{768} + 11 \text{Li}_4 \left(\frac{1}{2} \right) + \frac{11}{24} \ln^4(2) \right. \\
& + \frac{5}{16} \zeta(5) - \frac{275}{32} \zeta(4) + \frac{8913}{1024} \zeta(3) - \frac{11}{4} \zeta(2) \ln^2(2) \Big) + C_A C_F T_F^2 \left(-\frac{39259}{20736} \right. \\
& + 2 \text{Li}_4 \left(\frac{1}{2} \right) + \frac{1}{12} \ln^4(2) - \frac{37}{16} \zeta(4) + \frac{4343}{1536} \zeta(3) - \frac{1}{2} \zeta(2) \ln^2(2) \Big) + C_F^3 T_F \left(\frac{217}{768} \right. \\
& - \frac{15}{8} \zeta(5) + \frac{169}{256} \zeta(3) \Big) + C_F^2 T_F^2 \left(\frac{8951}{6912} - 4 \text{Li}_4 \left(\frac{1}{2} \right) - \frac{1}{6} \ln^4(2) + \frac{25}{8} \zeta(4) - \frac{595}{256} \zeta(3) \right. \\
& + \zeta(2) \ln^2(2) \Big) + C_F T_F^3 \left(\frac{359}{1944} - \frac{1}{3} \zeta(3) \right) + \frac{d_R^{abcd} d_R^{abcd}}{N_F} \left(\frac{1}{4} - \frac{15}{8} \zeta(3) \right) \Big] \ln \left(\frac{\mu^2}{m^2} \right) \\
& + \left[C_A^2 C_F T_F \left(\frac{19867}{13824} - \frac{33}{32} \zeta(3) \right) + C_A C_F^2 T_F \left(-\frac{219}{128} + \frac{33}{32} \zeta(3) \right) + C_A C_F T_F^2 \left(-\frac{2059}{6912} \right. \right.
\end{aligned}$$

$$\begin{aligned}
& + \frac{3}{8}\zeta(3) + \frac{15}{16}C_F^3T_F + C_F^2T_F^2\left(\frac{193}{2304} - \frac{3}{8}\zeta(3)\right) + \frac{31}{216}C_FT_F^3 \Big] \ln^2\left(\frac{\mu^2}{m^2}\right) \\
& + \left[\frac{17}{48}C_A^2C_FT_F - \frac{143}{384}C_AC_FT_F^2 - \frac{13}{48}C_AC_FT_F^2 + \frac{31}{192}C_F^2T_F^2 - \frac{5}{216}C_FT_F^3 \right] \ln^3\left(\frac{\mu^2}{m^2}\right) \\
& + \left[\frac{121}{2304}C_A^2C_FT_F - \frac{11}{192}C_AC_FT_F^2 + \frac{1}{128}C_F^2T_F^2 + \frac{1}{48}C_FT_F^3 \right] \ln^4\left(\frac{\mu^2}{m^2}\right) \\
& + n_l \left[C_AC_FT_F^2 \left(-\frac{5155}{31104} + 2\text{Li}_4\left(\frac{1}{2}\right) + \frac{1}{12}\ln^4(2) - \frac{43}{16}\zeta(4) + \frac{997}{576}\zeta(3) \right. \right. \\
& \left. \left. - \frac{1}{2}\zeta(2)\ln^2(2) \right) + C_F^2T_F^2 \left(\frac{319}{192} - 4\text{Li}_4\left(\frac{1}{2}\right) - \frac{1}{6}\ln^4(2) + \frac{7}{2}\zeta(4) - \frac{97}{32}\zeta(3) \right. \right. \\
& \left. \left. + \zeta(2)\ln^2(2) \right) - \frac{143}{648}C_FT_F^3 \right] \ln\left(\frac{\mu^2}{m^2}\right) + n_l^2 C_FT_F^3 \left(-\frac{3401}{7776} + \frac{7}{18}\zeta(3) \right) \ln\left(\frac{\mu^2}{m^2}\right) \\
& + n_l \left[-\frac{2581}{3456}C_AC_FT_F^2 - \frac{9}{64}C_F^2T_F^2 + \frac{283}{864}C_FT_F^3 \right] \ln^2\left(\frac{\mu^2}{m^2}\right) + \frac{31}{216}n_l^2 C_FT_F^3 \ln^2\left(\frac{\mu^2}{m^2}\right) \\
& + n_l \left[-\frac{13}{96}C_AC_FT_F^2 + \frac{1}{8}C_F^2T_F^2 \right] \ln^3\left(\frac{\mu^2}{m^2}\right) + n_l \left[-\frac{11}{288}C_AC_FT_F^2 \right. \\
& \left. + \frac{1}{48}C_FT_F^3 \right] \ln^4\left(\frac{\mu^2}{m^2}\right) + \frac{1}{144}n_l^2 C_FT_F^3 \ln^4\left(\frac{\mu^2}{m^2}\right) . \tag{32}
\end{aligned}$$

and

$$\zeta_1^{(2)} = \frac{5}{96}C_FT_F + \frac{89}{1152}C_AT_F - \left(\frac{1}{8}C_FT_F + \frac{5}{96}C_AT_F \right) \ln\left(\frac{\mu^2}{m^2}\right) + \frac{1}{32}C_AT_F \ln^2\left(\frac{\mu^2}{m^2}\right) , \tag{33}$$

$$\zeta_2^{(2)} = \frac{5}{96}C_FT_F - \frac{1}{8}C_FT_F \ln\left(\frac{\mu^2}{m^2}\right) , \tag{34}$$

$$\zeta_3^{(1)} = -\frac{1}{3}T_F \ln\left(\frac{\mu^2}{m^2}\right) , \tag{35}$$

$$\begin{aligned}
\tilde{\zeta}_1^{(3)} & = (1 - \xi^{(n_f)}) \left(C_A^2T_F \left(\frac{2039}{27648} - \frac{1}{48}\zeta(3) \right) - \frac{7}{144}C_A^2T_F \ln\left(\frac{\mu^2}{m^2}\right) \right. \\
& \left. + \frac{5}{384}C_A^2T_F \ln^2\left(\frac{\mu^2}{m^2}\right) - \frac{1}{384}C_A^2T_F \ln^3\left(\frac{\mu^2}{m^2}\right) \right) , \tag{36}
\end{aligned}$$

$$\tilde{\zeta}_3^{(1)} = -\frac{89}{1152}C_AT_F + \frac{5}{96}C_AT_F \ln\left(\frac{\mu^2}{m^2}\right) - \frac{1}{32}C_AT_F \ln^2\left(\frac{\mu^2}{m^2}\right) , \tag{37}$$

$$\zeta_{3g}^{(1)} = \frac{1}{3}T_F \ln\left(\frac{\mu^2}{m^2}\right) , \tag{38}$$

$$\zeta_{4g}^{(1)} = \frac{1}{3} T_F \ln \left(\frac{\mu^2}{m^2} \right) . \quad (39)$$

In these expression $m \equiv m(\mu)$ is the $\overline{\text{MS}}$ quark mass and $N_F = N_c$. Other variants with $\alpha_s^{(n_l)}$ and the on-shell heavy quark mass can be found in [33]. The colour factors are defined in Eq. (22).

References

- [1] K. G. Chetyrkin, B. A. Kniehl and M. Steinhauser, Nucl. Phys. B **510** (1998) 61 [hep-ph/9708255].
- [2] K. G. Chetyrkin, Nucl. Phys. B **710** (2005) 499 [hep-ph/0405193].
- [3] K. G. Chetyrkin and M. Steinhauser, Phys. Rev. Lett. **83** (1999) 4001 [hep-ph/9907509].
- [4] K. G. Chetyrkin and M. Steinhauser, Nucl. Phys. B **573** (2000) 617 [hep-ph/9911434].
- [5] K. Melnikov and T. v. Ritbergen, Phys. Lett. B **482** (2000) 99 [hep-ph/9912391].
- [6] P. Marquard, L. Mihaila, J. H. Piclum and M. Steinhauser, Nucl. Phys. B **773** (2007) 1 [hep-ph/0702185].
- [7] K. G. Chetyrkin, Phys. Lett. B **404** (1997) 161 [hep-ph/9703278].
- [8] J. A. M. Vermaseren, S. A. Larin and T. van Ritbergen, Phys. Lett. B **405** (1997) 327 [hep-ph/9703284].
- [9] T. van Ritbergen, J. A. M. Vermaseren and S. A. Larin, Phys. Lett. B **400** (1997) 379 [hep-ph/9701390].
- [10] M. Czakon, Nucl. Phys. B **710** (2005) 485 [hep-ph/0411261].
- [11] A. G. Grozin, M. Hoeschele, J. Hoff, M. Steinhauser, M. Hoeschele, J. Hoff and M. Steinhauser, JHEP **1109** (2011) 066 [arXiv:1107.5970 [hep-ph]].
- [12] V. P. Spiridonov, IYal-P-0378.
- [13] M. F. Zoller, JHEP **1604** (2016) 165 [arXiv:1601.08094 [hep-ph]].
- [14] M. Spira, JHEP **1610** (2016) 026 [arXiv:1607.05548 [hep-ph]].
- [15] J. Grigo, K. Melnikov and M. Steinhauser, Nucl. Phys. B **888** (2014) 17 [arXiv:1408.2422 [hep-ph]].
- [16] P. Nogueira, J. Comput. Phys. **105** (1993) 279.

- [17] R. Harlander, T. Seidensticker and M. Steinhauser, Phys. Lett. B **426** (1998) 125 [hep-ph/9712228].
- [18] T. Seidensticker, hep-ph/9905298.
- [19] <http://sfb-tr9.ttp.kit.edu/software/html/q2eexp.html>.
- [20] B. Ruijl, T. Ueda and J. Vermaseren, arXiv:1707.06453 [hep-ph].
- [21] T. van Ritbergen, A. N. Schellekens and J. A. M. Vermaseren, Int. J. Mod. Phys. A **14** (1999) 41 [hep-ph/9802376].
- [22] R. N. Lee, arXiv:1212.2685 [hep-ph].
- [23] R. N. Lee, J. Phys. Conf. Ser. **523** (2014) 012059 [arXiv:1310.1145 [hep-ph]].
- [24] A. V. Smirnov, Comput. Phys. Commun. **189** (2015) 182 [arXiv:1408.2372 [hep-ph]].
- [25] R. N. Lee and I. S. Terekhov, JHEP **1101** (2011) 068 [arXiv:1010.6117 [hep-ph]].
- [26] Y. Schroder and A. Vuorinen, JHEP **0506** (2005) 051 [hep-ph/0503209].
- [27] K. G. Chetyrkin, M. Faisst, C. Sturm and M. Tentyukov, Nucl. Phys. B **742** (2006) 208 [hep-ph/0601165].
- [28] R. N. Lee, private communication.
- [29] M. Steinhauser, Comput. Phys. Commun. **134** (2001) 335 [arXiv:hep-ph/0009029].
- [30] Y. Schroder and M. Steinhauser, JHEP **0601** (2006) 051 [hep-ph/0512058].
- [31] K. G. Chetyrkin, J. H. Kühn and C. Sturm, Nucl. Phys. B **744** (2006) 121 [hep-ph/0512060].
- [32] T. Liu and M. Steinhauser, Phys. Lett. B **746** (2015) 330 [arXiv:1502.04719 [hep-ph]].
- [33] <https://www.ttp.kit.edu/preprints/2018/ttp18-033/>.
- [34] T. Inami, T. Kubota and Y. Okada, Z. Phys. C **18** (1983) 69.
- [35] A. Djouadi, M. Spira and P. M. Zerwas, Phys. Lett. B **264** (1991) 440.
- [36] K. G. Chetyrkin, B. A. Kniehl and M. Steinhauser, Phys. Rev. Lett. **79** (1997) 353 [hep-ph/9705240].
- [37] M. Steinhauser, Phys. Rept. **364** (2002) 247 [hep-ph/0201075].
- [38] M. Kramer, E. Laenen and M. Spira, Nucl. Phys. B **511** (1998) 523 [hep-ph/9611272].
- [39] K. Chetyrkin, P. Baikov and J. Kühn, PoS LL **2016** (2016) 010.

- [40] P. A. Baikov, K. G. Chetyrkin and J. H. Kühn, Phys. Rev. Lett. **118** (2017) no.8, 082002 [arXiv:1606.08659 [hep-ph]].
- [41] F. Herzog, B. Ruijl, T. Ueda, J. A. M. Vermaseren and A. Vogt, JHEP **1702** (2017) 090 [arXiv:1701.01404 [hep-ph]].
- [42] T. Luthe, A. Maier, P. Marquard and Y. Schroder, JHEP **1710** (2017) 166 [arXiv:1709.07718 [hep-ph]].
- [43] M. F. Zoller and K. G. Chetyrkin, JHEP **1212** (2012) 119 [arXiv:1209.1516 [hep-ph]].
- [44] M. F. Zoller, JHEP **1410** (2014) 169 [arXiv:1407.6921 [hep-ph]].
- [45] C. Anastasiou, C. Duhr, F. Dulat, E. Furlan, T. Gehrmann, F. Herzog, A. Lazopoulos and B. Mistlberger, JHEP **1605** (2016) 058 [arXiv:1602.00695 [hep-ph]].
- [46] B. Mistlberger, JHEP **1805** (2018) 028 [arXiv:1802.00833 [hep-ph]].
- [47] P. Banerjee, S. Borowka, P. K. Dhani, T. Gehrmann, V. Ravindran, arXiv:1809.05388 [hep-ph].